Journal of the European Ceramic Society 22 (2002) 337–345

www.elsevier.com/locate/jeurceramsoc

Measurement of the t→m and m→t transformations in Ce–TZP by dilatometry and impedance spectroscopy

Andy Tiefenbach[a], Susanne Wagner[b,*], Rainer Oberacker[b], Bernd Hoffmann[a]

[a]*Institut für Werkstoffe der Elektrotechnik (IWE), Universität Karlsruhe (TH), Adenauerring 20, 76131 Karlsruhe, Germany*
[b]*Institut für Keramik im Maschinenbau (IKM), Universität Karlsruhe (TH), Haid und Neu-Straβe 7, 76131 Karlsruhe, Germany*

Received 23 November 2000; received in revised form 23 March 2001; accepted 28 April 2001

Abstract

The thermally induced t→m and m→t phase transformation of 9 mol% CeO_2-stabilized ZrO_2 with mean grain sizes varying from 1.2 to 2.7 μm has been characterized by dilatometry, XRD and impedance spectroscopy. XRD analysis indicates an increase in the volume fraction of the monoclinic phase from 0.69 to 0.89 with increasing grain size, which could be quantitatively correlated with the impedance spectra of the materials. Based on these findings, the m→t retransformation could be studied in situ by impedance spectroscopy in the temperature range from 20–350 °C. Depending on the grain size, the changes in the capacitive and resistive parts of the electrical impedance correlate well with the retransformation ranges obtained by dilatometry. Therefore, impedance spectroscopy is a useful analytical tool to study the transformation behaviour of zirconia ceramics. © 2001 Elsevier Science Ltd. All rights reserved.

Keywords: Grain growth; Impedance spectroscopy; Non-destructive evaluation; Phase transformation; TZP; ZrO_2

1. Introduction

Polycrystalline tetragonal zirconia ceramics (TZP) belong to the group of transformation toughened ceramics, which were developed during the last two decades. Meanwhile, they have found practical application in a variety of mechanical components, which are subjected to static or cyclic loads. Their increased toughness results mainly from a zone of inelastic deformation around the tip of propagating cracks, the so called process zone.[1,2] Triggered by the crack tip stress field, the metastable tetragonal (t) phase inside the process zone partially transforms to the stable monoclinic (m) symmetry. The Martensitic t→m transformation involves a dilatational strain of about 4% and a shear strain of about 16% and is usually accompanied by microcracking.[3] The consequence of this process is an increase in the work of fracture. The transformation toughening contribution ΔK^T is proportional to the square root of the height h of the process zone, which develops on both sides of a propagating crack.

Cracks in TZP are consequently surrounded by a more or less extended process zone containing monoclinic zirconia. Crack detection by non destructive testing methods, which is difficult in ceramics, could be facilitated if the cracks could be traced by the response of such process zones by methods with a sensitivity for phase composition. The present work is part of a more comprehensive research project,[4] which evaluates the potential of impedance spectroscopy (IS) for this purpose. There are some studies for the characterization of undamaged ceramics by impedance spectroscopy.[5–8] For the characterization of damaged material there is only limited information in literature. The effect of loaded cracks at high temperatures on the electrical properties has been studied on yttria stabilized zirconia.[9]

In particular, the present work deals with the detection of monoclinic phase constituents in Ce stabilized TZP (Ce–TZP) bulk materials by impedance spectroscopy. Ce–TZP was chosen for its high transformability, which allows to initiate the t→m transformation not only by external stresses, but also by cooling to moderate cryogenic temperatures. The thermally induced phase transformation behaviour of Ce–TZP is schematically shown in Fig. 1.[10]

* Corresponding author.
E-mail address: susanne.wagner@ikm.uni-karlsruhe.de (S. Wagner).

0955-2219/01/$ - see front matter © 2001 Elsevier Science Ltd. All rights reserved.
PII: S0955-2219(01)00286-2

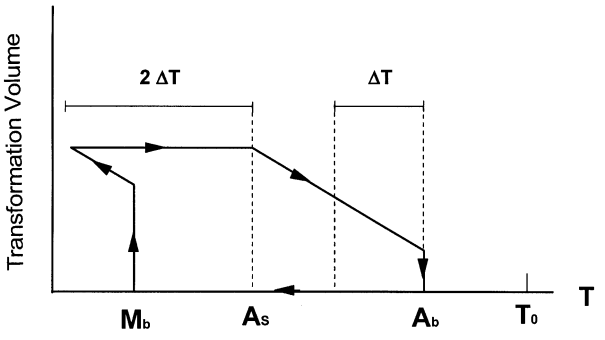

Fig. 1. Transformation curves for thermally induced t→m and m→t transformation in Ce–TZP (schematically [10]).

During cooling of the tetragonal phase, the t→m transformation starts spontaneously at the so-called Martensite burst-temperature M_b. A significant volume fraction of the material takes part in this autocatalytic transformation. Further cooling below M_b may result in a gradual increase in the transformed volume. Upon heating, the reverse m→t transformation begins at the Austenite (t) start temperature A_s and is completed by a burst like reaction at the Austenite burst temperature A_b. The transformation temperatures depend on the stabilizer content. They increase with the grain size of the material. Several mechanisms have been proposed to explain the grain size dependence of M_b. They include the nucleation process, which is favoured by a larger grain size[10] and local residual stresses, which promote the transformation.[11–13] The tetragonal phase shows a large anisotropy in cristallographic thermal expansion coefficient. This thermal anisotropy leads to high residual stresses after cooling which can be described by the relation.

$$\sigma_{TEA} = \Delta\alpha_{th}\Delta T d_k/r \quad (1)$$

where $\Delta\alpha_{th}$ is the difference in the thermal expansion, ΔT the temperature difference, d_k the grain size and r the distance from the triple point. According to this relation, the residual stresses are proportional to the grain size and so the transformation potential increases with increasing the grain size. This effect has been measured by different authors.[10,11] For 12 mol% ceria stabilized zirconia (12Ce–TZP) an increase of M_b from 175 to 250 K has been detected increasing the grain size of the ceramic from 1 to 8 μm.[11] The authors determined the transformation temperatures from the thermal expansion hysteresis using a dilatometer with a cooling chamber. The reverse transformation can be explained by the thermoelastic stability of the plate shaped monoclinic regions in the tetragonal matrix which are gradually reduced in thickness at temperatures beyond A_s and which become completely instable at A_b.[10]

In the present study the t→m transformation as well as the m→t retransformation of 9 mol% CeO_2 stabilized ZrO_2 (9Ce–TZP) has been characterized using dilatometry and impedance spectroscopy. This transformation behaviour has been investigated in dependence of the mean grain size of the 9Ce–TZP material. The grain size was varied by annealing the samples for different times. The results obtained by dilatometry, TEM, and XRD measurements will be correlated to changes in the electrical properties.

2. Experimental procedure

2.1. Sample preparation

For the sample preparation 9 mol% CeO_2 stabilized ZrO_2 powder (9Ce–TZP, Unitec, UK) has been used. Plates of 65×45×12 mm^3 were produced by pressing, cold isostatic repressing and sintering at 1400 °C for 2 h in air. In order to vary the grain size, subsequent annealing at 1400 °C in air for 16 to 256 h was carried out. The required specimen shapes were manufactured from the plates by diamond cutting and grinding. All specimens were annealed at 1200 °C for 1 h to remove residual stresses and the grinding induced monoclinic phase in the near surface region. This condition will be denoted in the following as the "initial state".

2.2. Phase transformation

By cooling the specimens down in cryogenic silicon oil, transformation of the tetragonal to monoclinic (m→t) phase was induced. The transformation strain was traced during cooling by strain gauges which were applied to the specimens. Cooling was carried out down to −85 °C, where all of the specimens had undergone their Martensitic burst reaction. The condition after t→m transformation and subsequent removing of the specimens out of the silicon oil back to ambient conditions is denoted the "transformed state".

After the specimens had been characterized, they were used to investigate the temperature induced m→t retransformation. Retransformation was studied in two ways:

1. Heating the specimens inside a dilatometer (Netzsch 402) at a heating rate of 2 K/min up to 400 °C.
2. Heating the specimens inside a furnace, coupled with an impedance spectroscope, up to 350 °C.

The corresponding condition will be denoted the "retransformed state".

2.3. Characterization of microstructure

Scanning (SEM) and transmission (TEM) electron microscopy were utilized for investigating the microstructure. The mean grain size was determined by the

line intercept method from SEM micrographs taken from polished and thermally etched specimens. Samples for TEM investigations were prepared by grinding, dimpling and ion milling. A Zeiss EM912 Omega microscope with an accelerating voltage of 120 kV was used for TEM investigations. The phase analysis was performed at an X-ray diffractometer (Siemens model D500) using Cu-K_α-radiation and a secondary graphite monocromator. The monoclinic fraction was derived from the intensities of the $(-111)_m$, $(111)_m$ and $(111)_t$ peaks according to the method described by Toraya et al.[14]

2.4. Electrical measurements

The electrical measurements were performed at specimens with a dimension of $10\times8\times12$ mm^3 using an impedance analyser (SI 1260, Solartron) in air. Electrodes required for the electrical measurements were prepared by vacuum deposition of platinum. At the so-contacted specimens impedance spectra were recorded over a frequency range from 1 Hz to 1 MHz at temperatures up to 350 °C. Heating of the samples was realized by high-intensity infrared line heaters.

At room temperature, the impedance spectra indicate exclusively capacitive behaviour in the investigated frequency range. In the temperature range between 200 to 300 °C, all spectra show essentially one capacitive range at high frequencies and one ohmic range at low frequencies. Thus, the spectra could be simulated simply by an electrical circuit with one R–C element[15] (this is shown in the experimental results in Fig. 7). The values of the circuit parameters R and C were obtained by least square fitting. From the capacitance C of this circuit, the capacitance c of the sample and the effective permeability ϵ_{eff} of the material were derived by:

$$c = C(L/A) \tag{2}$$

$$\varepsilon_{eff} = c/\varepsilon_0 \tag{3}$$

L denotes the length (10 mm) and A the cross-section (8×12 mm) of the specimens. The electrical conductance σ was calculated from the resistive part R of the impedance by:

$$\sigma = 1/R(L/A) \tag{4}$$

3. Results

3.1. Microstructure of the materials in the initial state

Fig. 2a shows a SEM micrograph of the sample annealed for 256 h at 1400 °C. No exaggerated grain growth could be observed. The shape of the grains and the width of their size distribution are not essentially changed compared to the as sintered microstructure.

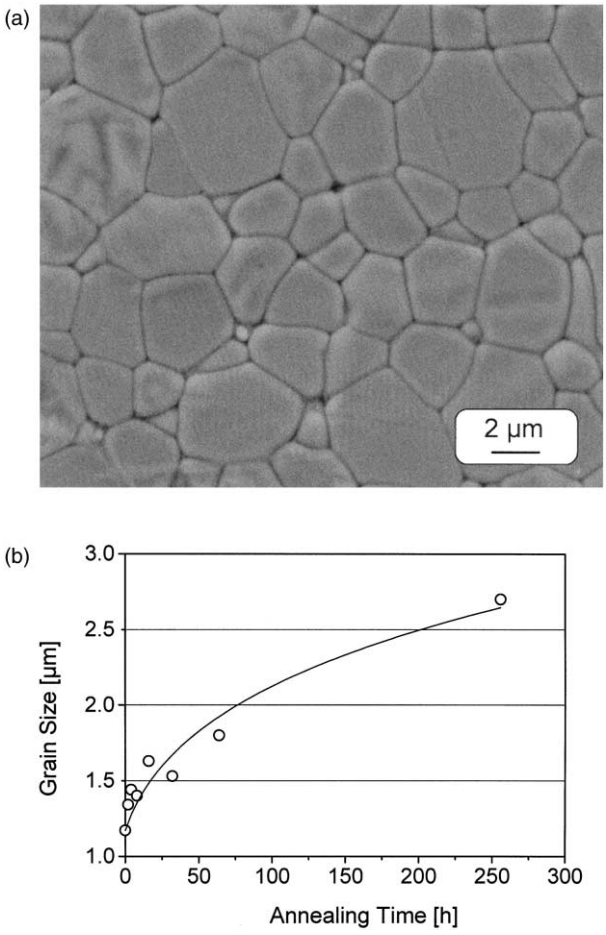

Fig. 2. (a) Microstructure of 9Ce–TZP after annealing for 256 h at 1400 °C; (b) grain size in 9Ce–TZP in dependence of the annealing time at 1400 °C.

The annealing treatment results, however, in significant grain coarsening, which can be characterized by the mean grain size d, represented as data points in Fig. 2b. They can be fitted by a common grain growth law[16] in the form of Eq. (5):

$$d^n - d_0^n = k\cdot t_g \tag{5}$$

where t_g is the annealing time, d_o is the initial grain size, k is a scaling constant and n is the grain growth exponent. A least square fit yields an exponent of $n=4$ and a scaling constant of $k=0.19$ µm^n/h.

A grain growth exponent of $n=4$ indicates grain boundary controlled grain growth of impure systems with a coalescence of a second phase by grain boundary diffusion. It correlates well with findings of Theunissen for a similar 9Ce–TZP.[17] The presence of a second phase has been detected in TEM investigations (Fig. 4a).

3.2. Thermally induced transformation behaviour of 9Ce–TZP

XRD measurements indicate a single phase tetragonal microstructure for the variations annealed up to 64 h, respectively with a grain size of up to 1.8 μm. In the material with the grain size of 2.7 μm, a monoclinic phase content of 30% was detected, induced during cooling of this material from the annealing temperature to room temperature (Table 1). Due to the large grain size, this material undergoes a partial t→m transformation in the near surface region on cooling from the stress relaxation treatment.

4. Temperature induced t→m transformation

During cooling the specimens to temperatures below room temperature, a spontaneous transformation of the tetragonal to the monoclinic phase at the Martensitic burst temperature M_b was detected from the Measurements of the transformation strain. Fig. 3 presents the measured transformation temperatures M_b as a function of the grain size. The material with the smallest grain size (1.2 μm) transforms at −60 °C, whereas the transformation temperature of the material with 2.7 μm grain size is −15 °C. The experiments show more or less a linear grain size dependence of the transformation temperature M_b on the grain size.

Quantitative XRD analysis indicate a fraction of the monoclinic phase of 70–90%, corresponding to a tetragonal fraction of 30–10%, after the cooling treatment (Table 1). The volume fraction of the monoclinic phase in the transformed materials increases monotonously with the grain size from 69% at 1.2 μm to 89% at 2.7 μm grain size. Transformation takes place almost completely at M_b. No significant increase in the monoclinic fraction was observed between samples cooled only to M_b and samples, which were further cooled down to −85 °C.

TEM micrographs of the microstructure in the initial state and after the t→m transformation treatment are represented in Fig. 4. They are in a good qualitative agreement with the XRD results. In the initial state, the material exhibits a single phase tetragonal microstructure with a grain boundary phase located in the triple points. No microcracks were detected in this condition. After the t→m transition, monoclinic as well as tetragonal grains are observed. Furthermore, microcracks have developed at the grain boundaries due to the volume increase during the t→m phase transition.

Table 1
Microstructure and electrical properties of 9Ce–TZP before and after cooling induced t→m transformation

Annealing time (h)	0	16	64	256
Mean grain size (μm)	1.2	1.6	1.8	2.7
Initial state				
XRD vol. fraction m (%)	0	0	0	0/30[a]
Eff. permittivity	38.1	38.9	38.6	38.4
After t→m transition				
XRD vol. fraction m (%)	69	78	83	89
Eff. permittivity	26.7	26.0	25.5	24.4

[a] Near surface region.

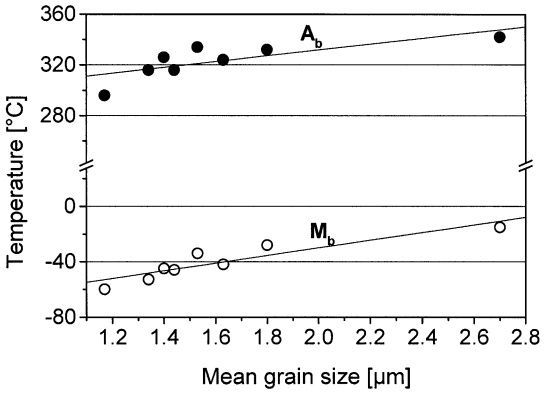

Fig. 3. Temperatures of the t→m transformation and m→t retransformation depending on the mean grain size.

4.1. Electrical properties

At room temperature only the capacitive part of the impedance can be measured, from which the effective permittivity ε_{eff} of the different materials was derived. ε_{eff} Of the tetragonal phase ranges from 38 to 39 and is essentially independent from the grain size, as can be seen from the materials annealed up to 64 h in Table 1. The permittivity of the material annealed for 256 h is at the same level, in spite of its high near surface monoclinic phase content. This indicates a very thin tetragonal/monoclinic surface layer of this material in the initial state, induced by cooling from the annealing temperature of 1400 °C to room temperature.

There is a reproducible, drastic decrease in the permittivity of all materials after the cooling induced t→m transformation as shown in Table 1. Differences of −30% for specimens with a grain size of 1.2 μm and of −36% for the material with the largest grain size of 2.7 μm have been measured. This shows that the cooling induced phase transformation occurs in the bulk of the materials and is not limited to near surface regions.

The effective permittivity after transformation decreases monotonously with increasing grain size. This is obviously caused by the higher monoclinic volume fraction in the coarser grained materials. In Fig. 5, the effective permittivity is plotted versus the tetragonal phase content measured by XRD. When the data are fitted by a linear regression, the extrapolation to 0% tetragonal phase yields an effective permittivity of the pure monoclinic material of $\varepsilon_m = 22.5$. Under physical aspects, a

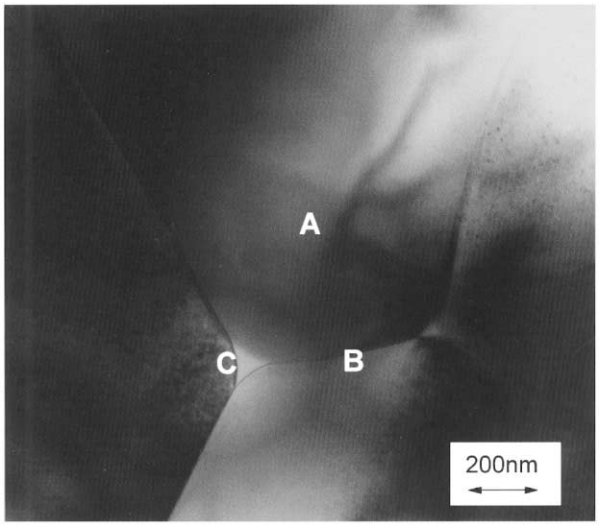

(a)

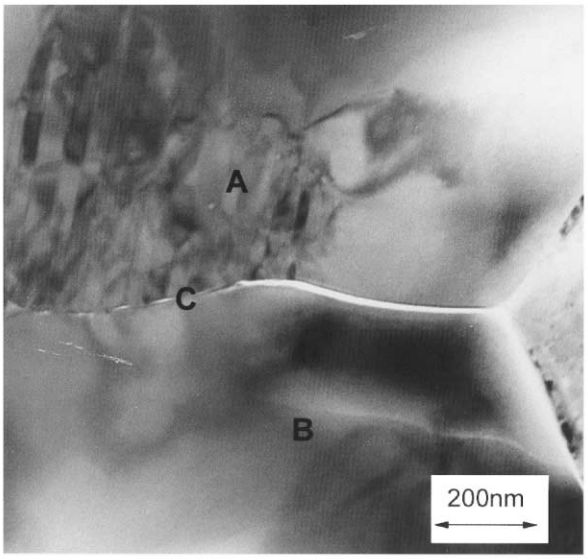

(b)

Fig. 4. (a) TEM micrograph of tetragonal zirconia (A) tetragonal grain, (B) grain boundary, (C) grain boundary phase in a triple point; (b) TEM micrograph of transformed zirconia with, (A) monoclinic grain, (B) tetragonal grain, (C) microcracks at the grain boundary induced by transformation.

linear relation represents a parallel connection of a tetragonal and a monoclinic layer, that means a parallel connection of two capacitors. The dashed and dotted curve in Fig. 5 were obtained using the Maxwell–Wagner relation as well as the series layer model, a serial connection of the two layers. The applicability of these models will be discussed in Section 6.

5. The m→t retransformation

Heating the transformed specimens beyond the Austenite temperature A_b, a m→t retransformation is

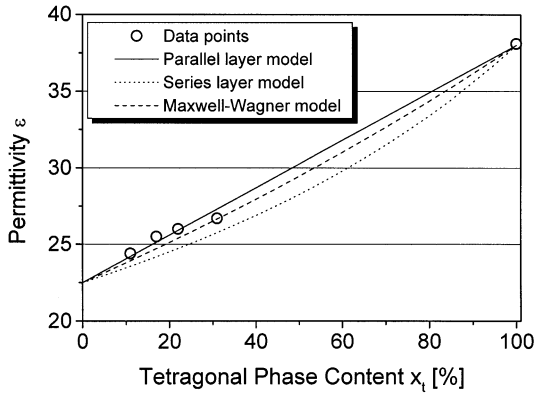

Fig. 5. Effective permittivity in dependence of the tetragonal phase content.

expected. The re-transformation m→t is known to take place over an extended temperature interval and causes a linear contraction of about 1%. However, the main part of the transformation reaction should occur close to A_b.

The volume decrease during transformation can be easily measured using dilatometry. Fig. 6 shows the dilatometer curves of the m→t retransformation for the materials with the different grain sizes. At 250 °C the retransformation process starts, first for the material with the smallest grains. The onset temperature A_s shifts to higher temperatures when the grain size increases. The Austenite temperature A_b increases from 296 to 342 °C increasing the grain size from 1.2 to 2.7 μm (Fig. 3). At a temperature of 350 °C, the retransformation process is completed for all investigated zirconia materials. This was confirmed by XRD measurements carried out after the dilatometer experiments.

The dilatometer curves show some differences in the relative length change during retransformation. For the 9Ce–TZP materials with a grain size $\leqslant$1.8 μm, the relative length change at the retransformation temperature increases with the grain size. This can be explained by the increasing volume fraction of monoclinic phase prior to the retransformation treatment. The measured contraction for the material with a grain size of 2.7 μm however is much smaller than the contraction of the other annealed samples, despite of its higher monoclinic phase fraction. The reason for this smaller contraction are probably crack face displacements, which hinder a complete crack closure during the m→t transformation.

5.1. Electrical properties

Besides dilatometry, impedance spectroscopy was applied to study the retransformation process. The electrical measurements were performed at temperatures up to 350 °C. In a first step, the materials with the different grain sizes were investigated in their initial (tetragonal) state. In the second step, the specimens after

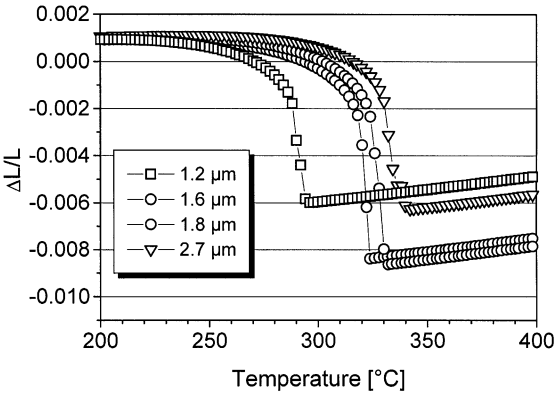

Fig. 6. Relative length change $\Delta L/L_0$ during heating of t→m transformed 9Ce–TZP.

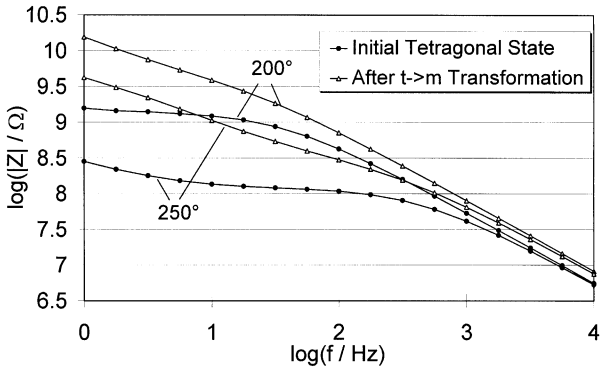

Fig. 7. Bode characteristics of 9Ce–TZP before and after t→m transformation at 200 and 250 °C for a grain size of 1.2 µm.

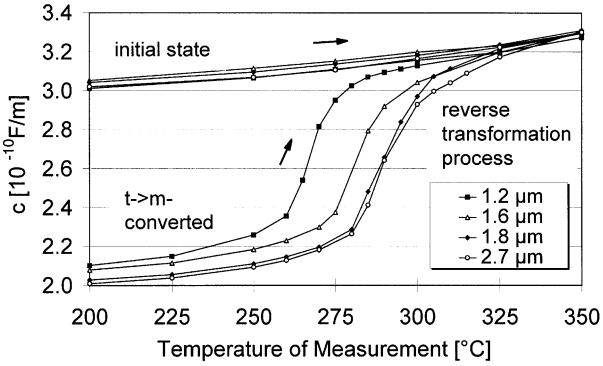

Fig. 8. Normalized capacitances of the materials in their initial (tetragonal) state and during the m→t retransformation after cooling induced t→m transition.

the cooling induced t→m transformation have been tested.

Fig. 7 compares the impedance spectra of specimens in the initial state and after t→m transformation at 200 and 250 °C in form of Bode plots. For the variations annealed up to 256 h, one obtains qualitatively similar spectra.

In the initial state one recognizes a capacitive transition region at low frequencies and an ohmic region over the mid-frequency range as well as a high-frequency capacitive field. As a consequence of the t→m transformation, the electrical properties change clearly. At high frequencies, there is still a purely capacitive behaviour. Compared to the initial state, the magnitude of the impedance is by far higher. Therefore, a reduced capacity determines the electrical behaviour. At lower frequencies, a superposition of ohmic and capacitive fields can be observed. The characteristics have higher magnitudes compared to the initial state. At low frequencies, one finds a dominating capacitive transition region. Furthermore, at 250 °C and frequencies between 10 and 1000 Hz, a field with a predominantly ohmic character is observed. Decreasing the temperature, this field shifts to lower frequencies. From these impedance spectra the normalized capacitance c and the normalized conductance σ were derived by a single R–C element simulation according to Section 2.

In Fig. 8 the normalized capacitance is plotted in dependence of the measurement temperature. Below 225 °C, the values of c for t→m transformed materials are clearly lower than in the corresponding, purely tetragonal initial states. Here, the lower permittivity of the predominantly monoclinic 9Ce–TZP materials takes effect. The value c decreases with increasing the volume fraction of the monoclinic phase or grain size, respectively. This correlates well with the results from the permittivity measurements at room temperature (see Table 1). With increasing temperature, the values of c then slowly increase for all materials. Depending on the grain size, the reverse m→t transformation starts beyond 225 °C. This leads to an increase of the capacitance. The largest capacitance gradients, which indicate the onset temperature of the reverse m→t transformation, shift to higher temperatures with increasing grain size. With continuing temperature increase, the normalized capacitance approaches asymptotically the corresponding value of the pure tetragonal materials. This indicates the completion of the retransformation process at temperatures, which are in good agreement with the dilatometer experiments.

The normalized conductance derived from the R–C simulation element is plotted in Fig. 9 versus the reciprocal temperature. The electrical conductance of the monoclinic and tetragonal phase differs significantly. In the Arrhenius plot the curves are characterized by three different intercepts. A first linear section at low temperatures, where the material is still predominantly monoclinic, is followed by a transition region where the m→t phase transformation takes place. With increasing grain size of the specimens, this transition region shifts to higher temperatures. Beyond 300 °C, all characteristics end in a second linear dependence, where finally all grains are tetragonal again. The grain size hardly affects conductivity outside of the transition regions. If one extrapolates the conductance of the tetragonal

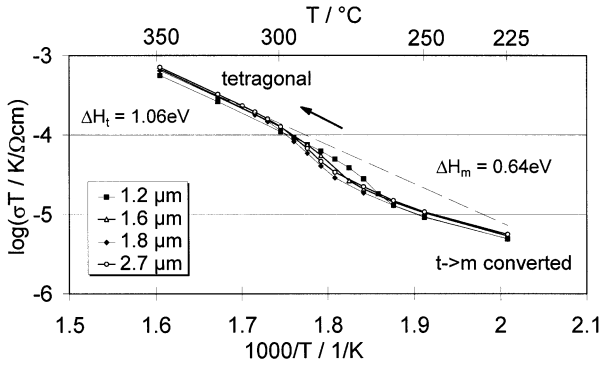

Fig. 9. Arrhenius plots of the normalized conductances of tetragonal grains and during the reverse m→t transformation of the t→m transformed materials depending on the reverse temperature for different grain sizes.

phase to lower temperatures, it is about 1.8 times higher than the measured conductance of the monoclinic grains. Also, the activation energy with 1.06 eV is significantly higher than that of the monoclinic phase with 0.64 eV.

6. Discussion

With respect to the grain size dependence of the transformation temperatures M_b and A_b, the results are in qualitative agreement with literature. The transformation temperatures of the investigated 9 mol% Ce–TZP are, however, much more sensitive to the grain size as it is the case for the 12 mol% TZP measured by Becher et al.[11] For the former, M_b increases from −60 to −15 °C for grain sizes of 1.2 and 2.7 μm, respectively. For the latter, the interval of grain size ranges from about 2 to 8 μm for a corresponding temperature interval. This has to be expected as a consequence of the different transformation entropy changes in the differently stabilized materials. The increasing M_b temperatures indicate an increasing transformation tendency, which also explains the higher monoclinic content with increasing grain size.

Impedance spectroscopy at room temperature indicates a drastic decrease of permittivity during the transformation of the tetragonal to the monoclinic phase in 9 mol% Ce–TZP from about 38 to 22.5. This is mainly caused by the change of crystal structure. Since all oxide ceramics are ionic crystals,[18] the differences in the lattice parameters and the different relocatability of the ions against each other take effect to the ionic polarization. This is the essential contribution to the total polarization[19] and finally it determines the effective permittivity of the material. The magnitude of this contribution is predominantly determined by the oscillator thickness of the ionic bonds.[20] A smaller influence on the permittivity decrease might also result from textures as well as from the air volume of opened cracks induced by volume extension after t→m transformation.

This effect could be used as a very simple non destructive method to detect phase transformations in TZP materials, which seems not to be recognized at present. Due to its significance, even quantitative phase analysis seems to be possible, as can be seen from Fig. 5. A linear relationship between ε_{eff} and the volume content of tetragonal phase is given by the parallel layer model[21] [Eq. (6)] where both, the monoclinic and the tetragonal layer, connect the two electrodes.

$$\varepsilon_{eff} = \varepsilon_m + x_t(\varepsilon_t - \varepsilon_m) \tag{6}$$

This linear relation is, however, not exactly justified, but an approximation of a linear relationship to 0% tetragonal phase should be adequate for the estimation of ε_m.

A physically better justified correlation between ε_{eff} and the volume content of tetragonal phase x_t can be derived from the Maxwell–Wagner model. Assuming a dispersion of spheres of tetragonal grains in a continuous medium of the monoclinic phase the following expression can be given as:[22,23]

$$\varepsilon_{eff} = \varepsilon_m \frac{\varepsilon_t + 2\varepsilon_m - 2x_t(\varepsilon_m - \varepsilon_t)}{\varepsilon_t + 2\varepsilon_m + x_t(\varepsilon_m - \varepsilon_t)} \tag{7}$$

The third model, which can be used for the estimation of the tetragonal volume content, is the series layer model, based on the relation:[21]

$$\varepsilon_{eff} = \varepsilon_m \frac{\varepsilon_m \cdot \varepsilon_t}{\varepsilon_t - x_t(\varepsilon_t - \varepsilon_m)} \tag{8}$$

On the basis of a permittivity of $\varepsilon_t = 38$ for the pure tetragonal and a permittivity of $\varepsilon_m = 22.5$ for the pure monoclinic material, the curves in Fig. 5 have been derived. It can be mentioned that the Maxwell–Wagner model and the parallel layer model correspond better to the measured values than the series layer model.

At enhanced temperatures, impedance spectroscopy provides two characteristic properties of the material: the normalized capacitance c and the normalized conductance σ. Both characteristics change significantly with the phase composition. The dilatometer experiments and impedance spectroscopy agree well with respect to the transformation behaviour, characterized by the Austenite temperature A_b. From the value of capacity determined experimentally from the impedance measurements, even quantitative relationships could be derived for the volume fractions of the monoclinic and tetragonal phase during the entire transformation process, e.g. by application of Eqs. (6)–(8). The conductance characteristics show different activation energies for the monoclinic and the tetragonal phase.

In the temperature range 200–300 °C only volume effects are detectable. That means the permittivity and

ionic conductivity of the grains predominantly influence the impedance spectra.[24] Cracks as well as grain boundaries are not detectable up to 300 °C. However, above 300 °C two ohmic and two capacitive ranges are observed in the impedance spectra. For a microstructural interpretation of this behaviour the brick layer model, a network with 2 *R–C* elements, can be used.[15,25] In the model the first ohmic range at low frequencies and the followed capacitive transition region can be assigned to the behaviour of the grain boundaries, whereas the high frequency range can be associated to the grains. In further work it has been demonstrated that cracks influence the low frequency range of these high temperature spectra.[26]

7. Conclusions

Comparing the electrical results with dilatometer and XRD measurements, the following statements can be derived:

1. The temperature ranges of the m→t retransformation of 9Ce–TZP materials measured by dilatometry correlate well with results of impedance spectroscopy. Both test methods show the same increase of the transformation temperature A_b with increasing grain size of the 9 mol% Ce–TZP samples.
2. The evaluation of the impedance spectra shows, that the permittivity and the electric conductivity of the monoclinic phase is significantly lower compared to the tetragonal phase. From permittivity measurements of t→m transformed material, the tetragonal as well as the corresponding monoclinic phase content can be estimated. If the grain size increases, the monoclinic phase fraction after the cooling induced t→m transition increases. These results agree quantitatively well with XRD measurements.

Thus, it can be stated, that impedance spectroscopy is a useful tool for the investigation of the transformation process in TZP ceramics.

Acknowledgements

This work was funded by the Deutsche Forschungsgemeinschaft (DFG) under contract Nos. Ho 693/11 and Ob 104/4.

References

1. Sun, Q., Zhao, Z., Chen, W., Qing, X., Xu, X. and Dai, F., Experimental study of stress-induced localised transformation plastic zones in tetragonal zirconia polycrystalline ceramics. *J. Am. Ceram. Soc.,* 1994, **77**(5), 1352–1356 .
2. Hannik, R., Kelly, P. and Muddle, B. C., Transformation toughening in zirconia-containing ceramics. *J. Am. Ceram. Soc.,* 2000, **83**(3), 461–487.
3. Chen, I. W., Model of transformation toughening in brittle materials. *J. Am. Ceram. Soc.,* 1991, **74**(10), 2564–2572.
4. Tiefenbach, A., Elektrische Charakterisierung mechanischer Schädigungen in ZrO_2-Keramik. VDI-Fortschrittsberichte, VDI-Verlag, Düsseldorf, 1999.
5. Bauerle, J. B., Study of solid electrolyte polarization by a complex admittance method. *J. Phys. Chem. Solid*, 1969, 2657–2670.
6. Kleitz, M., Bernard, H., Fernandez, E. and Schouler, E., Impedance spectroscopy and electrical resistance measurements on stabilized zirconia. In *Adv. in Ceramics 3. Science and Technology of Zirconia. Am. Ceram. Soc*., 1981, pp. 310–336.
7. Muccillo, E. N. and Kleitz, M., Impedance spectroscopy of Mg-partially-stabilized zirconia and cubic phase decomposition. *J. Eur. Ceram. Soc.,* 1996, **16**, 453–465.
8. Magistris, A. and Chiodelli, G., The dielectric responce of zirconia-based materials. Adv. in Ceramics 24B. In *Science and Technology of Zirconia III. Am. Ceram. Soc*., 1988, pp. 895–900.
9. Dessmond, L. and Kleitz, M., Effects of mechanical damage on the electrical properties of zirconia ceramics. *J. Eur. Ceram. Soc.,* 1992, **9**, 35–39.
10. Reyes-Morel, P. E., Cherng, J.-S. and Chen, I.-W., Transformation plasticity of CeO_2-stabilized tetragonal zirconia polycrystals: II, plseudoelasticity and shape memory effect. *J. Am. Ceram. Soc.,* 1988, **71**(8), 648–657.
11. Becher, P. F. and Swain, M. V., Grain-size-dependent transformation behavior in polycrystalline tetragonal zirconia. *J. Am. Ceram. Soc.,* 1992, **75**(3), 495–502.
12. Becher, P. F., Alexander, K. B., Bleier, A., Waters, S. B. and Warwick, W. H., Influence of ZrO_2 grain size and content on the transformation response in the Al_2O_3–ZrO_2 (12 mol% CeO_2) System. *J. Am. Ceram. Soc.,* 1993, **76**(3), 657–663.
13. Schmauder, S. and Schubert, H., Significance of internal stresses for the martensitic transformation in yttria-stabilized zirconia polycrystals during degradation. *J. Am. Ceram. Soc.,* 1986, **69**(7), 534–540.
14. Toraya, H., Yoshimura, M. and Somiya, S., Calibration curve for quantitative analysis of the monoclinic-tetragonal ZrO_2 system by X-ray diffraction. *J. Am. Ceram. Soc.,* 1984, **67**, 183–184.
15. Beekmans, N. M. and Heyne, L., Correlation between impedance, microstructure and composition of calcia-stabilized zirconia. *Electrochim. Acta,* 1976, **21**, 303–310.
16. Brook, R. J., Controlled grain growth. In *Treatise on Materials Science and Technology*. Vol. 9, ed. F. F. Y. Wang. Academic Press, New York, 1976, pp. 331–364.
17. Theunissen, G., *Microstructure, fracture toughness and strength of (ultra)fine-grained tetragonal zirconia ceramics*. PhD thesis, University Twente, Netherlands.
18. Waser, R., Hennings, D. and Baiatu, T., Die elektrischen Keramiken. In *Werkstoffe und Bauelemente der Elektrotechnik, Band 5: Keramik*. Teubner-Verlag, Stuttgart, 1994.
19. Salmang, H. and Scholze, H., *Keramik. Teil 1, 6*. Auflage, Springer-Verlag, Berlin, 1982.
20. Wersing, W., High frequency ceramic dielectrics and their application for microwave components. In *Electronic Ceramics*. Elsevier Applied Science, 1991, 67–119.
21. MacDonald, J. R., *Impedance Spectroscopy*. J. Wiley & Sons, New York, 1987.
22. Maxwell, J. C., *Electricity and Magnetism*, vol. 1. Clarendon Press, London, 1892.
23. Wagner, K. W., Explanation of the dielectric fatigue phenomenon on the basis of Maxwell's concept. *Archiv für Elektrotechnik*, Springer-Verlag, Berlin, 1914.

24. Barhmi, A., Schouler, E., Hammou, A. and Kleitz, M., Electrical properties of tetragonal partially stabilized zirconia. In *Advances in Ceramics*, Vol. 24B. *Am. Ceram. Soc*., 1988, pp. 885–894.
25. van Dijk, T. and Burggraaf, A. J., Grain boundary effects on ionic conductivity in ceramic $Gd_xZr_{1-x}O_{2-(x/2)}$ solid solutions. *Phys. Stat. Sol. (a)*, 1981, **63**, 229–240.
26. Tiefenbach, A. and Hoffmann, B., Influence of a crack on the electrical impedance of polycrystalline ceramics. *J. Eur. Ceram. Soc.,* 2000, **20**, 2079–2094.